JACS
JOURNAL OF THE AMERICAN CHEMICAL SOCIETY
pubs.acs.org/JACS
Communication

Photo-CIDNP-Enhanced ^{19}F NMR for Rapid Protein Conformation and Ligand Binding Analysis

Zhaofei Chai,*[,§] Weixuan Wang,[§] Qiong Wu,[§] Xiaoli Liu, Jiawen Chen, Yanqi Xu, Guohua Xu, Xiuchao Zhao, Xin Zhou, Ling Jiang, Maili Liu, and Conggang Li*

Cite This: J. Am. Chem. Soc. 2026, 148, 34051−34057
Read Online
ACCESS | Metrics & More | Article Recommendations | Supporting Information

ABSTRACT: ^{19}F NMR spectroscopy is a powerful probe of protein conformation and dynamics but is intrinsically limited by low sensitivity common to other NMR techniques. Here, we integrate photochemically induced dynamic nuclear polarization (photo-CIDNP) with genetically encoded ^{19}F labels to enhance sensitivity by up to 220-fold, enabling the detection of 100 nM protein within 6.5 min. This approach employs commercially available, cost-effective ^{19}F-labeled amino acid analogues and is broadly applicable to proteins ranging from 6.6 to 54.2 kDa. It allows rapid analysis of conformational changes and ligand binding in the low-micromolar range within minutes. Notably, it can readily characterize interactions with dissociation constants below 5 μM, which are challenging to access using conventional NMR. The combination of photo-CIDNP-induced sensitivity enhancement with the environmental responsiveness of ^{19}F NMR establishes a practical platform for protein structural and interaction studies.

Nuclear magnetic resonance (NMR) spectroscopy serves as a powerful tool for characterizing protein structure and dynamics. Coupled with selective isotope labeling strategies, it significantly simplifies spectral complexity and enables site-specific conformational tracking.[1,2] Nevertheless, sensitivity remains a fundamental limitation, rendering the detection of low-expression proteins or low-abundance conformational states time-consuming and often infeasible.[3] To overcome this constraint, hyperpolarization techniques, such as dynamic nuclear polarization (DNP), parahydrogen-induced polarization (PHIP), and signal amplification by reversible exchange (SABRE), have garnered increasing interest for their capacity to enhance NMR signal intensities by orders of magnitude. Despite these advances, most methods are primarily applicable to small molecules.[4−6] Achieving hyperpolarization for biomacromolecules like proteins and nucleic acids under mild, aqueous conditions without compromising their native structure and function continues to pose a significant challenge.[7−12]

Photochemically induced dynamic nuclear polarization (Photo-CIDNP) emerges as a promising technique for in situ substrate polarization via light-activated triplet-state sensitizers under ambient conditions, offering advantages in both biocompatibility and instrumental simplicity.[13,14] Traditionally, the methodology has been applied to investigate protein folding and surface accessibility.[15−19] Recent optimizations in pulse sequences and polarization systems have extended its application to metabolite identification and fragment screening.[20−24] However, to explore its potential for protein signal enhancement, novel detection schemes are still needed to overcome the limitations of conventional ^{1}H NMR, such as signal overlap and low polarization efficiency. ^{1}H-detected ^{13}C hyperpolarization offers a promising approach for improved spectral resolution and signal enhancement, with its primary implementation challenge lying in the specialized and costly synthesis that ideally requires position-specific ^{13}C labels.[25−28]

The ^{19}F nucleus is a highly attractive candidate for photo-CIDNP studies. It exhibits high sensitivity to its local chemical environment, enabling high-resolution conformational analysis via 1D spectra while circumventing polarization transfer losses and the need for expensive isotopic labeling.[29−32] Furthermore, substituting ^{1}H with ^{19}F in organic radicals typically leads to higher electron spin density at the same position, resulting in larger hyperfine coupling constants and consequently, greater induced nuclear spin polarization.[19,33] Nevertheless, ^{19}F-based polarization systems remain relatively unexplored, and the development of highly efficient polarization platforms is urgently needed to unlock the full potential of this approach for protein structural biology.[34−38]

Herein, we demonstrated an up to 220-fold signal-to-noise enhancement (SNE) in proteins by employing commercially available fluorinated amino acids as efficient photo-CIDNP-active ^{19}F probes. Leveraging the boosted ^{19}F NMR, we enabled rapid detection of protein conformational changes and their interactions with substrates or drug ligands in low micromolar concentration ($\leq$5 μM). The combination of versatile ^{19}F probes with high-sensitivity photo-CIDNP is anticipated to substantially broaden the applicability of this technique in biomacromolecule studies.

Received: May 12, 2026
Revised: July 1, 2026
Accepted: August 4, 2026
Published: August 8, 2026

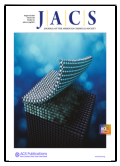

https://doi.org/10.1021/jacs.6c09740
J. Am. Chem. Soc. 2026, 148, 34051−34057

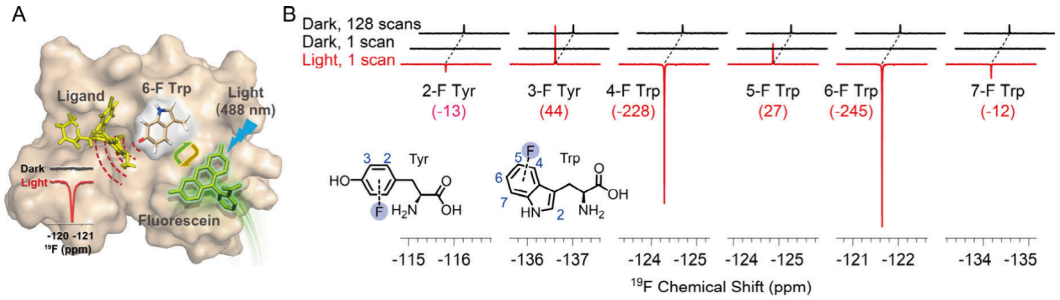

Figure 1. (A) Schematic illustration for the polarization of ^{19}F probe. The fluorescein undergoes reversible photochemical reaction with the ^{19}F probe, generating polarization via the radical-pair mechanism. The resulting sensitivity-enhanced ^{19}F NMR enables the monitoring of protein events, such as ligand binding. (B) ^{19}F NMR spectra of monofluorinated Trp and Tyr (30 μM) in the presence of fluorescein (10 μM). All spectra were acquired in photo-CIDNP buffer under illumination with a fiber-coupled 488 nm laser (1.28 W, 1.5 s) and are normalized to the same noise level hereafter (Supporting Information). The numbers in parentheses denote SNEs, where the negative sign indicates emission peaks.

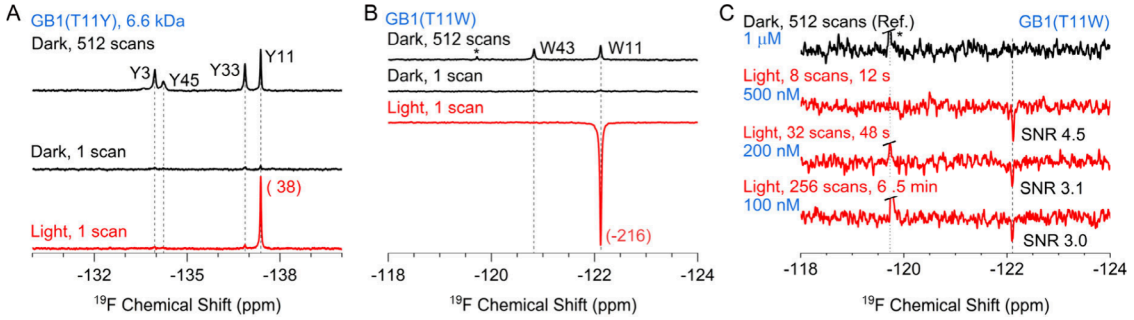

Figure 2. ^{19}F NMR spectra of GB1 labeled with (A) 3-F Tyr (125 μM) or 6-F Trp at (B) 125 μM and (C) sub-1 μM concentrations. No photo-CIDNP activity was observed for endogenous Trp and Tyr residues. *Signal from F^- ion.

While Tyr and Trp are established as efficient photo-CIDNP probes, the optimal site of fluorination for polarization remains unclear.[39] We therefore first tested their monofluorinated analogs using the commonly employed polarization reagent flavin mononucleotide (FMN). Our prior work suggested that the ^{19}F polarization efficiency at different sites could be predicted from the radical's ^{19}F spin density.[24] Density functional theory (DFT) calculations indicated that the spin densities on ^{19}F spins followed the order 6-*F* > 4-*F* > 7-*F* > 5-*F* for monofluorinated Trp radicals, and 3-*F* > 2-*F* for monofluorinated Tyr radicals (Tables S1 and S2), in good agreement with the experimental results (Figures S1−S3). Nevertheless, even the best-performing analogs, 3-F Tyr and 6-F Trp, exhibited only moderate SNEs for low-concentration samples (30 μM), showing enhancements of 12-fold and 36-fold, respectively. This limited polarization is consistent with the inefficiency of FMN for low-concentration samples (<100 μM), a consequence of its short triplet-state lifetime.[40,41]

We then selected fluorescein (FL) as the sensitizer for its favorable polarization performance for low-concentration samples.[42] Under identical irradiation conditions, the overall SNEs obtained with FL were significantly higher than those with FMN (Figure 1). Using 6-F Trp as an example, the ^{19}F NMR signal intensity increased linearly with concentration (R^2 > 0.99) within the 1−60 μM range and gradually saturated at concentrations exceeding 120 μM (Figures S4−S6). Both 6-F Trp and 3-F Tyr exhibited substantial SNEs of 245-fold and 44-fold, respectively. Interestingly, 5-F Trp (SNE 27-fold) demonstrated better polarization performance than 7-F Trp (SNE 12-fold), a trend that contrasted with the order predicted by their respective ^{19}F spin densities. This discrepancy can likely be attributed to differences in photo-reaction kinetics resulting from the lower oxidative ability of FL compared to FMN.[43] For comparison, the photo-CIDNP enhanced signal-to-noise ratios (SNRs) and corresponding SNEs for aromatic ^{1}H spins were lower than those for ^{19}F spins at identical molecular sites, despite the higher Larmor frequencies of ^{1}H spins on the same 700 MHz spectrometer (Figures S7, S8). The appreciable SNEs of 3-F Tyr and 6-F Trp with FL at low concentrations prompted us to explore their applicability in proteins.

Previous studies have demonstrated the efficient incorporation of monofluorinated Trp/Tyr analogs into proteins via metabolic labeling.[19,44−48] We first evaluated their polarization performance in proteins by mutating the highly dynamic residue T11 in model protein GB1 (*streptococcus* protein G B1 domain) into Trp or Tyr (Figures S9−S11),[49] thereby providing an identical microenvironment for both probes. The resulting variants showed high SNEs of 216-fold for 6-F Trp and 38-fold for 3-F Tyr, closely approaching the level of free-state probes (Figure 2). Notably, GB1(T11W) achieved a detection limit (SNR ≥ 3) of 200 nM with 32 scans, and 100 nM with 256 scans, constituting one of the highest sensitivities reported to date for solution NMR of proteins.[4]

We then turned to the SH3 (N-terminal SH3 domain of *Drosophila melanogaster* Drk), containing endogenous Trp (W36) and Tyr (Y52, Y37) residues (Figure 3).[50] The folded and unfolded states could be readily resolved in ^{19}F NMR spectra for both probes. Upon illumination, all ^{19}F spins exhibited polarized NMR signals. For 6-F Trp-labeled SH3, both states remained discernible at a concentration as low as 1.0 μM (256 scans; Figure S12), comparable to the sensitivity for ^{13}C-Trp-labeled SH3.[26] However, the incorporated ^{19}F probes exhibited lower SNEs (50 ∼ 70-fold for 6-F Trp and 6

https://doi.org/10.1021/jacs.6c09740
J. Am. Chem. Soc. 2026, 148, 34051−34057

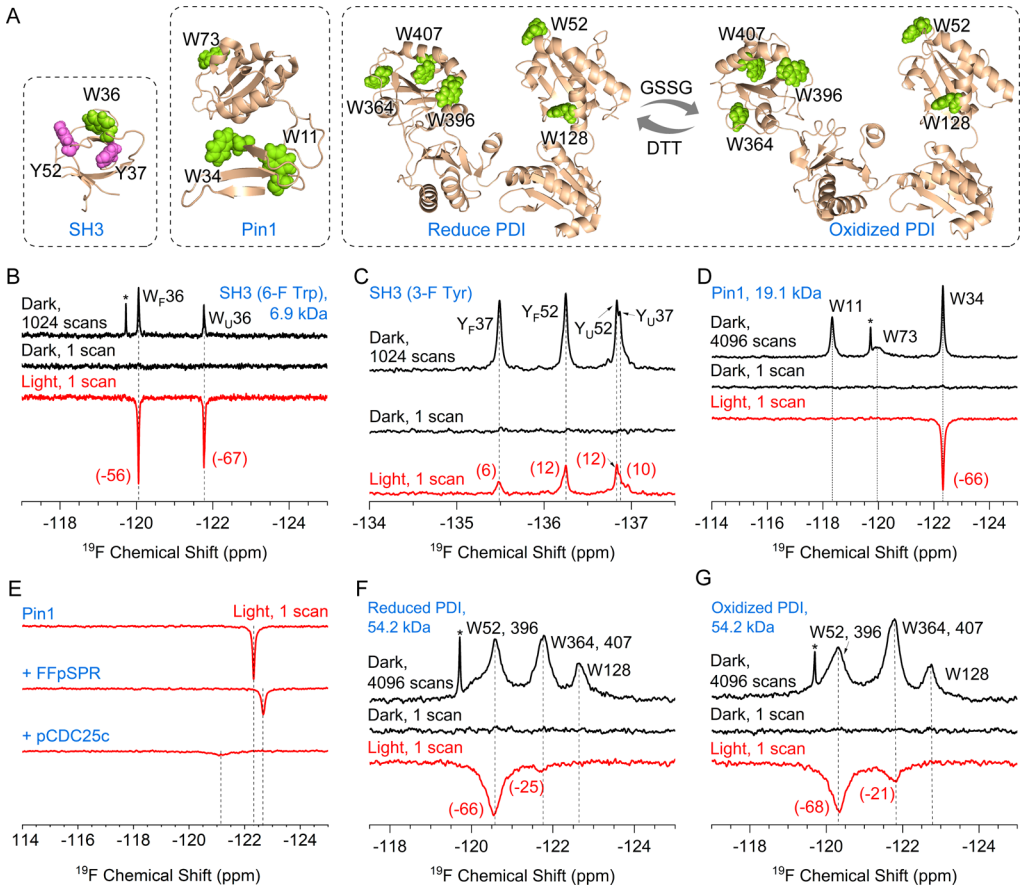

Figure 3. (A) Structures of SH3 (PDB: 2A36), Pin1 (PDB: 1NMV), reduced PDI (PDB: 4EKZ) and oxidized PDI (PDB: 4EL1), highlighting Trp (green) /Tyr (pink) residues. (B, C) ^{19}F NMR spectra of SH3 labeled with 6-F Trp or 3-F Tyr (125 μM). (D, E) ^{19}F NMR spectra of 6-F Trp-labeled Pin1 and its substrate-bound complexes (125 μM). (F, G) ^{19}F NMR spectra of reduced and oxidized states of 6-F Trp-labeled PDI (125 μM). Spectral assignments are provided in Supporting Information (Figures S15−S18).

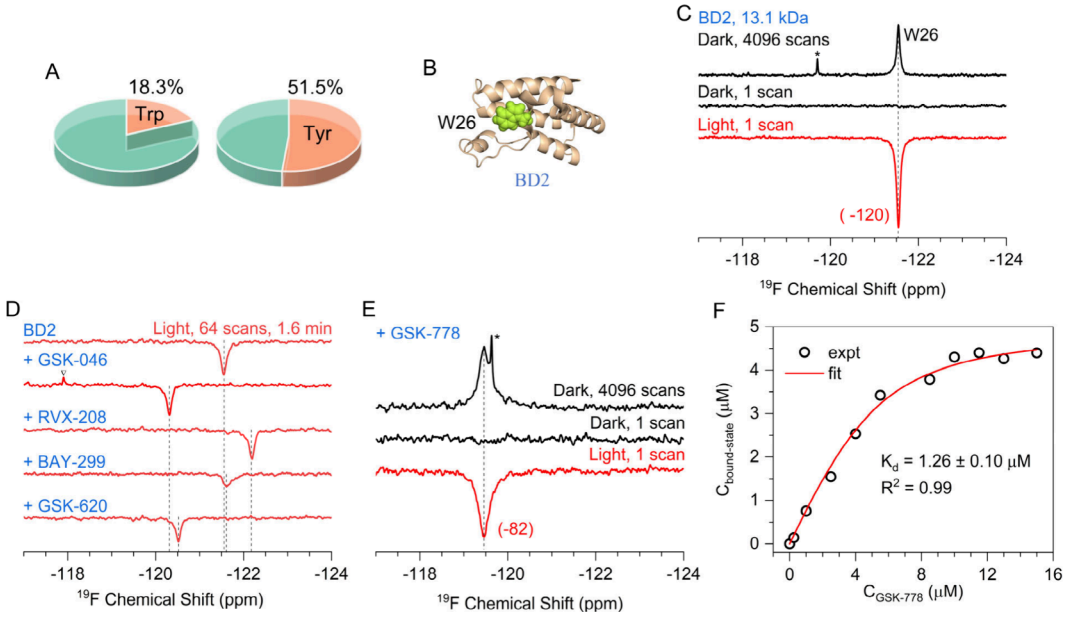

Figure 4. (A) Proportion of ligand-binding pockets containing Trp or Tyr residues (data source: PDBbind Database, v2020).[55] (B) Structure of BD2 (PDB: 7USK). (C) ^{19}F NMR spectra of 6-F Trp-labeled BD2 (125 μM). (D) ^{19}F NMR spectra of 6-F Trp-labeled BD2 (5 μM) in the presence of different ligands. (E) ^{19}F NMR spectra of 6-F Trp-labeled BD2 (125 μM) in the presence of GSK-778. (F) Titration of 6-F Trp-labeled BD2 (5 μM) with GSK-778. ▽Signal from the ligand.

https://doi.org/10.1021/jacs.6c09740
J. Am. Chem. Soc. 2026, 148, 34051−34057

~ 12-fold for Tyr) than those in GB1. This attenuation primarily results from reduced FL collision probability due to limited solvent-accessible surface area, unfavorable electrostatics, and side-chain orientation (Figure S13, S14, Table S3). Reduced dye accessibility was more pronounced in the folded state, as evidenced by unfolded-state SNEs equaling (Y52) or exceeding (W36, Y37) those of the folded state. These findings confirm that both 3-F-Tyr and 6-F-Trp function as photo-CIDNP probes under FL-mediated polarization, though 3-F-Tyr exhibits significantly lower polarization efficiency due to differences in radical pair dynamics.[51] Subsequent studies were accordingly centered on 6-F Trp.

To evaluate its broader applicability, we next applied the polarization system to larger proteins: Pin1 (peptidyl-prolyl isomerase NIMA-interacting 1, 19.1 kDa) and PDI (human protein disulfide-isomerase, 54.2 kDa). Pin1 contains one Trp (W73) residue in its PPIase domain and two additional Trp (W11 and W34) residues in its WW domain.[52] Upon illumination, only W34 exhibited polarized NMR signal with a SNE of 66-fold. Its location in the substrate-binding WW domain renders W34 a sensitive probe for monitoring binding events. Upon addition of two phosphorylated substrates, FFpSPR and pCDC25c,[53] the ^{19}F signals of W34 were broadened and shifted from −122.3 to −122.7 and −121.1 ppm, respectively. As these substrates themselves lack photo-CIDNP-active units, the decreased SNEs (39-fold for FFpSPR and 53-fold for pCDC25c, Figure S19), likely due to reduced dye accessibility to W34 upon substrate binding, serves as an additional indicator of microenvironmental change, complementing information from chemical shift and line shape.

PDI, characterized by its two -CGHC- redox-active motifs, contains tryptophan residues (W52, W396) proximal to these sites.[54] The two ^{19}F-labeled Trp residues, which exhibited identical chemical shifts, could function as sensitive reporters of protein redox state, displaying a 0.25 ppm downfield shift upon addition of oxidized glutathione. Both states displayed significant polarization, with SNEs exceeding 66-fold. For this medium-sized protein, conventional detection at 125 μM required 4096 scans (1.5 h) to achieve a SNR of 5.2, whereas the photo-CIDNP technique achieved a comparable SNR of 5.3 in a single scan (2 s), dramatically reducing the acquisition time. But the ^{19}F signals of the W364 and W407 residues showed moderate enhancements (~20-fold) and were insensitive to the redox state. These results demonstrated that photo-CIDNP-enhanced ^{19}F NMR provided a sensitive and rapid method for detecting protein conformational changes, prompting by its potential generality, an evaluation of its utility for drug discovery.

A database analysis revealed that a substantial proportion of ligand-binding pockets contain photo-CIDNP-polarizable residues, such as Trp and Tyr (Figure 4), suggesting the potential of photo-CIDNP-enhanced ^{19}F NMR for protein-based drug screening. This method directly provides structural information regarding the ligand binding site and allosteric effects, while traditionally requires high protein concentrations for sufficient SNR.[56] We demonstrated this approach using BD2 domain of BRD4 (bromodomain-containing protein 4), which contains a solvent-accessible Trp (W26) located around the region of high interest for current drug design.[57] 6-F Trp-labeled BD2 showed an intense signal (line-width: 0.10 ppm) with a high SNE of 120-fold. Upon adding potential ligands (RVX-208,[58] BAY-299,[59] GSK-620,[60] and GSK-046[61]), significant changes in chemical shift, line shape, and signal intensity were observed, even at 5 μM protein with only 64 scans, substantially lowering the typical requirement for protein concentration (>100 μM) and acquisition time. Compared to ligand-polarization-based screening,[20−22] our method accommodates ligands without photo-CIDNP-active moieties (Figures S20, S21), and for photo-CIDNP-silent cases, allosteric effects can in principle be harnessed via Trp mutations at proximal sites to generate reporters for conformational changes,[2] collectively expanding the applicability of photo-CIDNP-based screening.

Moreover, photo-CIDNP technology holds promise for measuring binding affinities of protein complexes with dissociation constants (K_D) below 5 μM—a range where traditional NMR methods often require substantial time or lack sufficient sensitivity. For example, after binding GSK-778, 6-F Trp-labeled BD2 showed a broadened resonance (line-width: 0.29 ppm) with a downfield shift of 2.1 ppm. The binding ligand (not photo-CIDNP-active, Figure S22) reduced FL accessibility, resulting in a lower SNE of 82-fold. By monitoring ^{19}F signal intensity, we determined a K_D of approximately 1.26 μM for this complex, consistent with the reported value (0.67 μM by TR-FRET assays).[61]

In summary, we have systematically investigated the polarization performance of ^{19}F at distinct sites within the aromatic rings of Tyr and Trp, establishing the 6-F Trp/FL combination as a highly efficient polarization system. This cost-effective system achieves signal enhancements exceeding 200-fold for proteins, enabling photo-CIDNP-enhanced ^{19}F NMR spectroscopy to rapidly detect protein conformational changes within minutes at low-micromolar concentrations (≤5 μM). We anticipate that further advances in the development of efficient polarizing reagents (e.g., for Tyr, His, and Met) and targetable substrates will broaden the method's applicability, particularly for high-throughput fragment screening integrated with automated platforms.[21,62]

■ ASSOCIATED CONTENT

Supporting Information

The Supporting Information is available free of charge at https://pubs.acs.org/doi/10.1021/jacs.6c09740.

Experimental procedures and supplementary figures (PDF)

■ AUTHOR INFORMATION

Corresponding Authors

Zhaofei Chai − *State Key Laboratory of Magnetic Resonance Spectroscopy and Imaging, National Center for Magnetic Resonance in Wuhan, Wuhan National Laboratory for Optoelectronics, Wuhan Institute of Physics and Mathematics, Innovation Academy for Precision Measurement Science and Technology, Chinese Academy of Sciences, Wuhan 430071, China; Graduate University of Chinese Academy of Sciences, Beijing 100049, China*; Email: czfei@wipm.ac.cn

Conggang Li − *State Key Laboratory of Magnetic Resonance Spectroscopy and Imaging, National Center for Magnetic Resonance in Wuhan, Wuhan National Laboratory for Optoelectronics, Wuhan Institute of Physics and Mathematics, Innovation Academy for Precision Measurement Science and Technology, Chinese Academy of Sciences, Wuhan 430071, China; Graduate University of Chinese Academy of Sciences, Beijing 100049, China*; orcid.org/0000-0002-5798-1722; Email: conggangli@wipm.ac.cn

https://doi.org/10.1021/jacs.6c09740
J. Am. Chem. Soc. 2026, 148, 34051−34057

Authors

Weixuan Wang − *State Key Laboratory of Magnetic Resonance Spectroscopy and Imaging, National Center for Magnetic Resonance in Wuhan, Wuhan National Laboratory for Optoelectronics, Wuhan Institute of Physics and Mathematics, Innovation Academy for Precision Measurement Science and Technology, Chinese Academy of Sciences, Wuhan 430071, China; Graduate University of Chinese Academy of Sciences, Beijing 100049, China*

Qiong Wu − *State Key Laboratory of Magnetic Resonance Spectroscopy and Imaging, National Center for Magnetic Resonance in Wuhan, Wuhan National Laboratory for Optoelectronics, Wuhan Institute of Physics and Mathematics, Innovation Academy for Precision Measurement Science and Technology, Chinese Academy of Sciences, Wuhan 430071, China; Graduate University of Chinese Academy of Sciences, Beijing 100049, China*

Xiaoli Liu − *State Key Laboratory of Magnetic Resonance Spectroscopy and Imaging, National Center for Magnetic Resonance in Wuhan, Wuhan National Laboratory for Optoelectronics, Wuhan Institute of Physics and Mathematics, Innovation Academy for Precision Measurement Science and Technology, Chinese Academy of Sciences, Wuhan 430071, China; Graduate University of Chinese Academy of Sciences, Beijing 100049, China*

Jiawen Chen − *State Key Laboratory of Magnetic Resonance Spectroscopy and Imaging, National Center for Magnetic Resonance in Wuhan, Wuhan National Laboratory for Optoelectronics, Wuhan Institute of Physics and Mathematics, Innovation Academy for Precision Measurement Science and Technology, Chinese Academy of Sciences, Wuhan 430071, China; Graduate University of Chinese Academy of Sciences, Beijing 100049, China*

Yanqi Xu − *State Key Laboratory of Magnetic Resonance Spectroscopy and Imaging, National Center for Magnetic Resonance in Wuhan, Wuhan National Laboratory for Optoelectronics, Wuhan Institute of Physics and Mathematics, Innovation Academy for Precision Measurement Science and Technology, Chinese Academy of Sciences, Wuhan 430071, China; Graduate University of Chinese Academy of Sciences, Beijing 100049, China*

Guohua Xu − *State Key Laboratory of Magnetic Resonance Spectroscopy and Imaging, National Center for Magnetic Resonance in Wuhan, Wuhan National Laboratory for Optoelectronics, Wuhan Institute of Physics and Mathematics, Innovation Academy for Precision Measurement Science and Technology, Chinese Academy of Sciences, Wuhan 430071, China; Graduate University of Chinese Academy of Sciences, Beijing 100049, China*

Xiuchao Zhao − *State Key Laboratory of Magnetic Resonance Spectroscopy and Imaging, National Center for Magnetic Resonance in Wuhan, Wuhan National Laboratory for Optoelectronics, Wuhan Institute of Physics and Mathematics, Innovation Academy for Precision Measurement Science and Technology, Chinese Academy of Sciences, Wuhan 430071, China; Graduate University of Chinese Academy of Sciences, Beijing 100049, China*

Xin Zhou − *State Key Laboratory of Magnetic Resonance Spectroscopy and Imaging, National Center for Magnetic Resonance in Wuhan, Wuhan National Laboratory for Optoelectronics, Wuhan Institute of Physics and Mathematics, Innovation Academy for Precision Measurement Science and Technology, Chinese Academy of Sciences, Wuhan 430071, China; Graduate University of Chinese Academy of Sciences, Beijing 100049, China*

Ling Jiang − *State Key Laboratory of Magnetic Resonance Spectroscopy and Imaging, National Center for Magnetic Resonance in Wuhan, Wuhan National Laboratory for Optoelectronics, Wuhan Institute of Physics and Mathematics, Innovation Academy for Precision Measurement Science and Technology, Chinese Academy of Sciences, Wuhan 430071, China; Graduate University of Chinese Academy of Sciences, Beijing 100049, China;* orcid.org/0000-0002-8505-8679

Maili Liu − *State Key Laboratory of Magnetic Resonance Spectroscopy and Imaging, National Center for Magnetic Resonance in Wuhan, Wuhan National Laboratory for Optoelectronics, Wuhan Institute of Physics and Mathematics, Innovation Academy for Precision Measurement Science and Technology, Chinese Academy of Sciences, Wuhan 430071, China; Graduate University of Chinese Academy of Sciences, Beijing 100049, China;* orcid.org/0000-0002-9359-915X

Complete contact information is available at: https://pubs.acs.org/10.1021/jacs.6c09740

Author Contributions

[§]The manuscript was written through contributions of all authors. All authors have given approval to the final version of the manuscript. These authors contributed equally.

Notes

The authors declare no competing financial interest.

■ ACKNOWLEDGMENTS

This work was supported by the Strategic Priority Research Program of the Chinese Academy of Sciences (XDB0540000), the National Natural Science Foundation of China (U25D8019 and 22574165), the National Key Research and Development Program of China (2023YFA1506500) and the CAS Project for Young Scientists in Basic Research (YSBR-068).

■ REFERENCES

(1) Arthanari, H.; Takeuchi, K.; Dubey, A.; Wagner, G. Emerging Solution NMR Methods to Illuminate the Structural and Dynamic Properties of Proteins. *Curr. Opin. Struc. Biol.* **2019**, *58*, 294−304.

(2) Shimada, I.; Ueda, T.; Kofuku, Y.; Eddy, M. T.; Wuthrich, K. GPCR Drug Discovery: Integrating Solution NMR Data with Crystal and Cryo-EM Structures. *Nat. Rev. Drug Discovery* **2019**, *18* (1), 59−82.

(3) Ardenkjaer-Larsen, J.-H.; Boebinger, G. S.; Comment, A.; Duckett, S.; Edison, A. S.; Engelke, F.; Griesinger, C.; Griffin, R. G.; Hilty, C.; Maeda, H.; Parigi, G.; Prisner, T.; Ravera, E.; van Bentum, J.; Vega, S.; Webb, A.; Luchinat, C.; Schwalbe, H.; Frydman, L. Facing and Overcoming Sensitivity Challenges in Biomolecular NMR Spectroscopy. *Angew. Chem., Int. Ed.* **2015**, *54* (32), 9162−9185.

(4) Eills, J.; Budker, D.; Cavagnero, S.; Chekmenev, E. Y.; Elliott, S. J.; Jannin, S.; Lesage, A.; Matysik, J.; Meersmann, T.; Prisner, T.; Reimer, J. A.; Yang, H.; Koptyug, I. V. Spin Hyperpolarization in Modern Magnetic Resonance. *Chem. Rev.* **2023**, *123* (4), 1417−1551.

(5) Lee, J. H.; Okuno, Y.; Cavagnero, S. Sensitivity Enhancement in Solution NMR: Emerging Ideas and New Frontiers. *J. Magn. Reson.* **2014**, *241*, 18−31.

(6) Posthumus, T. B.; Engelke, U. F. H.; Aspers, R. L. E. G.; Merx, J.; Boltje, T. J.; Martens, J.; Wevers, R. A.; Feiters, M. C.; Rutjes, F. P. J. T.; Tessari, M. Semi-Targeted Nuclear Magnetic Resonance Metabolomics via Parahydrogen-Induced Hyperpolarization for

Enhanced Sensitivity to Metabolic Composition. *J. Am. Chem. Soc.* **2025**, *147* (36), 33185−33192.
(7) Hilty, C.; Kurzbach, D.; Frydman, L. Hyperpolarized Water as Universal Sensitivity Booster in Biomolecular NMR. *Nat. Protoc.* **2022**, *17* (7), 1621−1657.
(8) Zachrdla, M.; Turhan, E.; Buckova, M.; Hansel-Hertsch, R.; Trantirek, L.; Kurzbach, D. Hyperpolarized NMR Reveals Low-Populated Folding Intermediates in DNA. *J. Am. Chem. Soc.* **2025**, *147* (50), 46563−46572.
(9) Epasto, L. M.; Che, K.; Kozak, F.; Selimovic, A.; Kaderavek, P.; Kurzbach, D. Toward Protein NMR at Physiological Concentrations by Hyperpolarized Water-Finding and Mapping Uncharted Conformational Spaces. *Sci. Adv.* **2022**, *8* (31), No. eabq5179.
(10) Movellan, K. T.; Zhu, W.; Banks, D.; Kempf, J.; Runge, B.; Gronenborn, A. M.; Polenova, T. Expanding the Tool Box for Native Structural Biology: ^{19}F Dynamic Nuclear Polarization with Fast Magic angle Spinning. *Sci. Adv.* **2024**, *10* (40), No. eadq3115.
(11) Lins, J.; Miloslavina, Y. A.; Avrutina, O.; Theiss, F.; Hofmann, S.; Kolmar, H.; Buntkowsky, G. Enhancing Sensitivity of Nuclear Magnetic Resonance in Biomolecules: Parahydrogen-Induced Hyperpolarization in Synthetic Disulfide-Rich Miniproteins. *J. Am. Chem. Soc.* **2024**, *146* (51), 35175−35184.
(12) Brandis, D.; Turhan, E.; Zachrdla, M.; Kurzbach, D. Residue-Resolved Liquid-State Hyperpolarized NMR of Peptide Condensate Surfaces. *J. Am. Chem. Soc.* **2025**, *147* (40), 36920−36927.
(13) Okuno, Y.; Cavagnero, S. Photochemically Induced Dynamic Nuclear Polarization: Basic Principles and Applications. *eMagRes.* **2017**, *6*, 283−314.
(14) Morozova, O. B.; Ivanov, K. L. Time-Resolved Chemically Induced Dynamic Nuclear Polarization of Biologically Important Molecules. *ChemPhysChem* **2019**, *20* (2), 197−215.
(15) Kaptein, R.; Dijkstra, K.; Nicolay, K. Laser Photo-CIDNP as a Surface Probe for Proteins in Solution. *Nature* **1978**, *274* (5668), 293−294.
(16) Mok, K. H.; Kuhn, L. T.; Goez, M.; Day, I. J.; Lin, J. C.; Andersen, N. H.; Hore, P. J. A Pre-Existing Hydrophobic Collapse in the Unfolded State of an Ultrafast Folding Protein. *Nature* **2007**, *447* (7140), 106−109.
(17) Im, J.; Lee, J.; Lee, J. H. Surface Accessibility of an Intrinsically Disordered Protein Probed by 2D Time-Resolved Laser-Assisted NMR Spectroscopy. *J. Am. Chem. Soc.* **2022**, *144* (37), 17010−17021.
(18) Lyon, C. E.; Jones, J. A.; Redfield, C.; Dobson, C. M.; Hore, P. J. Two-Dimensional ^{15}N−^{1}H Photo-CIDNP as a Surface Probe of Native and Partially Structured Proteins. *J. Am. Chem. Soc.* **1999**, *121* (27), 6505−6506.
(19) Khan, F.; Kuprov, I.; Craggs, T. D.; Hore, P. J.; Jackson, S. E. ^{19}F NMR Studies of the Native and Denatured States of Green Fluorescent Protein. *J. Am. Chem. Soc.* **2006**, *128* (33), 10729−10737.
(20) Bütikofer, M.; Stadler, G. R.; Kadavath, H.; Cadalbert, R.; Torres, F.; Riek, R. Rapid Protein−Ligand Affinity Determination by Photoinduced Hyperpolarized NMR. *J. Am. Chem. Soc.* **2024**, *146* (26), 17974−17985.
(21) Torres, F.; Bütikofer, M.; Stadler, G. R.; Renn, A.; Kadavath, H.; Bobrovs, R.; Jaudzems, K.; Riek, R. Ultrafast Fragment Screening Using Photo-Hyperpolarized (CIDNP) NMR. *J. Am. Chem. Soc.* **2023**, *145* (22), 12066−12080.
(22) Stadler, G. R.; Segawa, T. F.; Bütikofer, M.; Decker, V.; Loss, S.; Czarniecki, B.; Torres, F.; Riek, R. Fragment Screening and Fast Micromolar Detection on a Benchtop NMR Spectrometer Boosted by Photoinduced Hyperpolarization. *Angew. Chem., Int. Ed.* **2023**, *62* (40), No. e202308692.
(23) Kuhn, L. T.; Weber, S.; Bargon, J.; Parella, T.; Pérez-Trujillo, M. Hyperpolarization-Enhanced NMR Spectroscopy of Unaltered Biofluids Using Photo-CIDNP. *Anal. Chem.* **2024**, *96* (1), 102−109.
(24) Chai, Z.; Wang, W.; Chen, J.; Wu, Q.; Ma, L.; Liu, Z.; Xu, G.; Jiang, L.; Shu, Y.; Liu, M.; Li, C. Expanding the Molecular Scope of Photo-CIDNP for Nanomolar ^{19}F NMR Detection of Amines. *J. Am. Chem. Soc.* **2026**, *148* (9), 9213−9218.
(25) Lee, J. H.; Sekhar, A.; Cavagnero, S. ^{1}H-Detected ^{13}C Photo-CIDNP as a Sensitivity Enhancement Tool in Solution NMR. *J. Am. Chem. Soc.* **2011**, *133* (21), 8062−8065.
(26) Okuno, Y.; Mecha, M. F.; Yang, H.; Zhu, L.; Fry, C. G.; Cavagnero, S. Laser- and Cryogenic Probe-Assisted NMR Enables Hypersensitive Analysis of Biomolecules at Submicromolar Concentration. *Proc. Natl. Acad. Sci. U.S.A.* **2019**, *116* (24), 11602−11611.
(27) Yang, H.; Li, S.; Mickles, C. A.; Guzman-Luna, V.; Sugisaki, K.; Thompson, C. M.; Dang, H. H.; Cavagnero, S. Selective Isotope Labeling and LC-Photo-CIDNP Enable NMR Spectroscopy at Low-Nanomolar Concentration. *J. Am. Chem. Soc.* **2022**, *144* (26), 11608−11619.
(28) Shapla, U. M.; Smith, J. L.; Halder, A.; Thompson, L.; Buller, A. R.; Cavagnero, S. Highly Sensitive Detection of Tyrosine and Neurotransmitters by Stereoselective Biosynthesis and Photochemically Induced Dynamic Nuclear Polarization. *J. Am. Chem. Soc.* **2025**, *147* (46), 42361−42374.
(29) Divakaran, A.; Kirberger, S. E.; Pomerantz, W. C. K. SAR by (Protein-Observed) ^{19}F NMR. *Acc. Chem. Res.* **2019**, *52* (12), 3407−3418.
(30) Gronenborn, A. M. Small, but Powerful and Attractive: ^{19}F in Biomolecular NMR. *Structure* **2022**, *30* (1), 6−14.
(31) Kitevski-LeBlanc, J. L.; Prosser, R. S. Current Applications of ^{19}F NMR to Studies of Protein Structure and Dynamics. *Prog. Nucl. Magn. Reson. Spectrosc.* **2012**, *62*, 1−33.
(32) Luchinat, E.; Banci, L. In-Cell NMR: Recent Progresses and Future Challenges. *Rend. Lincei-Sci. Fis.* **2023**, *34* (3), 653−661.
(33) Schmidt, A.; Ayekoi, A.; Illarionov, B.; Fischer, M.; Bacher, A.; Weber, S. Transient ^{19}F Photo-CIDNP: A Practical Tool to Distinguish Intermediate Radical Species and Determine Isotropic Hyperfine Coupling Constants of ^{19}F Nuclei. *J. Chem. Phys.* **2025**, *162* (5). DOI: 10.1063/5.0246273
(34) Smith, M. J.; Bramham, J. E.; Nilsson, M.; Morris, G. A.; Castañar, L.; Golovanov, A. P. Lighting up Spin Systems: Enhancing Characteristic ^{1}H Signal Patterns of Fluorinated Molecules. *Chem. Commun.* **2023**, *59* (78), 11692−11695.
(35) Kuprov, I.; Hore, P. J. Chemically Amplified ^{19}F−^{1}H Nuclear Overhauser Effects. *J. Magn. Reson.* **2004**, *168* (1), 1−7.
(36) Bramham, J. E.; Golovanov, A. P. Sample Illumination Device Facilitates In Situ Light-Coupled NMR Spectroscopy without Fibre Optics. *Commun. Chem.* **2022**, *5* (1), 90.
(37) Gomez, M. V.; Baas, S.; Velders, A. H. Multinuclear 1D and 2D NMR with ^{19}F-Photo-CIDNP Hyperpolarization in a Microfluidic Chip with Untuned Microcoil. *Nat. Commun.* **2023**, *14* (1), 3885.
(38) Mompeán, M.; Sánchez-Donoso, R. M.; de la Hoz, A.; Saggiomo, V.; Velders, A. H.; Gomez, M. V. Pushing Nuclear Magnetic Resonance Sensitivity Limits with Microfluidics and Photo-Chemically Induced Dynamic Nuclear Polarization. *Nat. Commun.* **2018**, *9* (1), 108.
(39) Goez, M. Photo-CIDNP Spectroscopy. *Annu. Rep. NMR Spectrosc.* **2009**, *66*, 77−147.
(40) Lee, J. H.; Cavagnero, S. A Novel Tri-Enzyme System in Combination with Laser-Driven NMR Enables Efficient Nuclear Polarization of Biomolecules in Solution. *J. Phys. Chem. B* **2013**, *117* (20), 6069−6081.
(41) Fritz, B. J.; Matsui, K.; Kasai, S.; Yoshimura, A. Triplet Lifetimes of Some Flavins. *Photochem. Photobiol.* **1987**, *45* (4), 539−541.
(42) Okuno, Y.; Cavagnero, S. Fluorescein: A Photo-CIDNP Sensitizer Enabling Hypersensitive NMR Data Collection in Liquids at Low Micromolar Concentration. *J. Phys. Chem. B* **2016**, *120* (4), 715−723.
(43) Romero, N. A.; Nicewicz, D. A. Organic Photoredox Catalysis. *Chem. Rev.* **2016**, *116* (17), 10075−10166.
(44) Chai, Z.; Li, C. In-Cell ^{19}F NMR of Proteins: Recent Progress and Future Opportunities. *Chem.—Eur. J.* **2024**, *30* (23), No. e202303988.

(45) Crowley, P. B.; Kyne, C.; Monteith, W. B. Simple and Inexpensive Incorporation of ^{19}F-Tryptophan for Protein NMR Spectroscopy. *Chem. Commun.* **2012**, *48* (86), 10681−10683.
(46) Li, C.; Wang, G.-F.; Wang, Y.; Creager-Allen, R.; Lutz, E. A.; Scronce, H.; Slade, K. M.; Ruf, R. A. S.; Mehl, R. A.; Pielak, G. J. Protein ^{19}F NMR in Escherichia Coli. *J. Am. Chem. Soc.* **2010**, *132* (1), 321−327.
(47) Pham, L. B. T.; Costantino, A.; Barbieri, L.; Calderone, V.; Luchinat, E.; Banci, L. Direct Expression of Fluorinated Proteins in Human Cells for ^{19}F In-Cell NMR Spectroscopy. *J. Am. Chem. Soc.* **2023**, *145* (2), 1389−1399.
(48) Qianzhu, H.; Abdelkader, E. H.; Otting, G.; Huber, T. Genetic Encoding of Fluoro-l-tryptophans for Site-Specific Detection of Conformational Heterogeneity in Proteins by NMR Spectroscopy. *J. Am. Chem. Soc.* **2024**, *146* (19), 13641−13650.
(49) Chai, Z.; Wu, Q.; Cheng, K.; Liu, X.; Zhang, Z.; Jiang, L.; Zhou, X.; Liu, M.; Li, C. Visualizing Proteins in Human Cells at Near-Physiological Concentrations with Sensitive ^{19}F NMR Chemical Tags. *Angew. Chem., Int. Ed.* **2023**, *62* (22), No. e202300318.
(50) Evanics, F.; Bezsonova, I.; Marsh, J.; Kitevski, J. L.; Forman-Kay, J. D.; Prosser, R. S. Tryptophan Solvent Exposure in Folded and Unfolded States of an SH3 Domain by ^{19}F and ^{1}H NMR. *Biochemistry* **2006**, *45* (47), 14120−14128.
(51) Sobol, A.; Torres, F.; Aicher, A.; Renn, A.; Riek, R. Atto Thio 12 as a Promising Dye for Photo-CIDNP. *J. Chem. Phys.* **2019**, *151* (23), No. 234201.
(52) Luh, L. M.; Hansel, R.; Lohr, F.; Kirchner, D. K.; Krauskopf, K.; Pitzius, S.; Schafer, B.; Tufar, P.; Corbeski, I.; Guntert, P.; Dotsch, V. Molecular Crowding Drives Active Pin1 into Nonspecific Complexes with Endogenous Proteins Prior to Substrate Recognition. *J. Am. Chem. Soc.* **2013**, *135* (37), 13796−13803.
(53) Born, A.; Soetbeer, J.; Henen, M. A.; Breitgoff, F.; Polyhach, Y.; Jeschke, G.; Vogeli, B. Ligand-Specific Conformational Change Drives Interdomain Allostery in Pin1. *Nat. Commun.* **2022**, *13* (1), 4546.
(54) Richards, K. L.; Rowe, M. L.; Hudson, P. B.; Williamson, R. A.; Howard, M. J. Combined Ligand-Observe ^{19}F and Protein-Observe ^{15}N,^{1}H-HSQC NMR Suggests Phenylalanine as the Key Δ-Somatostatin Residue Recognized by Human Protein Disulfide Isomerase. *Sci. Rep.* **2016**, *6* (1), 19518.
(55) Wang, R.; Fang, X.; Lu, Y.; Wang, S. The PDBbind Database: Collection of Binding Affinities for Protein−Ligand Complexes with Known Three-Dimensional Structures. *J. Med. Chem.* **2004**, *47* (12), 2977−2980.
(56) Buchholz, C. R.; Pomerantz, W. C. K. ^{19}F NMR Viewed Through Two Different Lenses: Ligand-Observed and Protein-Observed ^{19}F NMR Applications for Fragment-Based Drug Discovery. *RSC Chem. Biol.* **2021**, *2* (5), 1312−1330.
(57) Liu, Z.; Wang, P.; Chen, H.; Wold, E. A.; Tian, B.; Brasier, A. R.; Zhou, J. Drug Discovery Targeting Bromodomain-Containing Protein 4. *J. Med. Chem.* **2017**, *60* (11), 4533−4558.
(58) Picaud, S.; Wells, C.; Felletar, I.; Brotherton, D.; Martin, S.; Savitsky, P.; Diez-Dacal, B.; Philpott, M.; Bountra, C.; Lingard, H.; Fedorov, O.; Muller, S.; Brennan, P. E.; Knapp, S.; Filippakopoulos, P. RVX-208, An Inhibitor of BET Transcriptional Regulators with Selectivity for the Second Bromodomain. *Proc. Natl. Acad. Sci. U.S.A.* **2013**, *110* (49), 19754−19759.
(59) Bouche, L.; Christ, C. D.; Siegel, S.; Fernandez-Montalvan, A. E.; Holton, S. J.; Fedorov, O.; Ter Laak, A.; Sugawara, T.; Stockigt, D.; Tallant, C.; Bennett, J.; Monteiro, O.; Diaz-Saez, L.; Siejka, P.; Meier, J.; Putter, V.; Weiske, J.; Muller, S.; Huber, K. V. M.; Hartung, I. V.; Haendler, B. Benzoisoquinolinediones as Potent and Selective Inhibitors of BRPF2 and TAF1/TAF1L Bromodomains. *J. Med. Chem.* **2017**, *60* (9), 4002−4022.
(60) Seal, J. T.; Atkinson, S. J.; Aylott, H.; Bamborough, P.; Chung, C.-w.; Copley, R. C. B.; Gordon, L.; Grandi, P.; Gray, J. R. J.; Harrison, L. A.; Hayhow, T. G.; Lindon, M.; Messenger, C.; Michon, A.-M.; Mitchell, D.; Preston, A.; Prinjha, R. K.; Rioja, I.; Taylor, S.; Wall, I. D.; Watson, R. J.; Woolven, J. M.; Demont, E. H. The Optimization of a Novel, Weak Bromo and Extra Terminal Domain (BET) Bromodomain Fragment Ligand to a Potent and Selective Second Bromodomain (BD2) Inhibitor. *J. Med. Chem.* **2020**, *63* (17), 9093−9126.
(61) Gilan, O.; Rioja, I.; Knezevic, K.; Bell, M. J.; Yeung, M. M.; Harker, N. R.; Lam, E. Y. N.; Chung, C.-w.; Bamborough, P.; Petretich, M.; Urh, M.; Atkinson, S. J.; Bassil, A. K.; Roberts, E. J.; Vassiliadis, D.; Burr, M. L.; Preston, A. G. S.; Wellaway, C.; Werner, T.; Gray, J. R.; Michon, A.-M.; Gobbetti, T.; Kumar, V.; Soden, P. E.; Haynes, A.; Vappiani, J.; Tough, D. F.; Taylor, S.; Dawson, S.-J.; Bantscheff, M.; Lindon, M.; Drewes, G.; Demont, E. H.; Daniels, D. L.; Grandi, P.; Prinjha, R. K.; Dawson, M. A. Selective Targeting of BD1 and BD2 of the BET Proteins in Cancer and Immunoinflammation. *Science* **2020**, *368* (6489), 387−394.
(62) Li, Z.; Wang, Y.; Wu, W.; Zhai, Z.; Cao, S. H.; Song, K.; Liu, Z.; Yan, A.; Sun, H.; Chen, Z. Multiwavelength Light-Emitting Diode-Array-Embedded Nuclear Magnetic Resonance System: A Non-invasive In Situ Platform for Hyperpolarization and Photochemical Analysis. *Anal. Chem.* **2026**, *98* (1), 476−487.

https://doi.org/10.1021/jacs.6c09740
J. Am. Chem. Soc. 2026, 148, 34051−34057